

# **QCD Predictions for Charm and Bottom Production at RHIC**

**R. Vogt**

**Nuclear Science Division, Lawrence Berkeley National Laboratory, Berkeley, CA  
94720, USA**

**Physics Department, University of California, Davis, CA 95616, USA**

**In collaboration with M. Cacciari and P. Nason, hep-ph/0502203**

# Charm as a Probe of Heavy Ion Collisions

Hard probe produced in the initial nucleon-nucleon collisions

Interacts strongly so its momentum can be modified by collisions during the evolution of the system leading to effects such as

- Energy loss in dense matter (Djordjevic et al, Lin et al, Kharzeev and Dokshitzer)
- Transverse momentum broadening due to hadronization from quark-gluon plasma (Svetitsky) or cold nuclear matter
- Collective flow of charm quarks (Lin and Molnar, Rapp et al)

In addition, if multiple  $c\bar{c}$  pairs are produced in a given event, can enhance  $J/\psi$  (hidden charm) production (Thews et al)

$pp$  and d+Au collisions serve as an important baseline for understanding medium effects on charm production, need good theoretical background and up-to-date open charm data

# Calculating Heavy Flavors in Perturbative QCD

‘Hard’ processes have a large scale in the calculation that makes perturbative QCD applicable: high momentum transfer,  $\mu^2$ , high mass,  $m$ , high transverse momentum,  $p_T$ , since  $m \neq 0$ , heavy quark production is a ‘hard’ process

Asymptotic freedom assumed to calculate the interactions between two hadrons on the quark/gluon level but the confinement scale determines the probability of finding the interacting parton in the initial hadron

Factorization assumed between the perturbative hard part and the universal, non-perturbative parton distribution functions

Hadronic cross section in an  $AB$  collision where  $AB = pp, pA$  or nucleus-nucleus is

$$\sigma_{AB}(S, m^2) = \sum_{i,j=q,\bar{q},g} \int_{4m_Q^2/s}^1 \frac{d\tau}{\tau} \int dx_1 dx_2 \delta(x_1 x_2 - \tau) f_i^A(x_1, \mu_F^2) f_j^B(x_2, \mu_F^2) \hat{\sigma}_{ij}(s, m^2, \mu_F^2, \mu_R^2)$$

$f_i^A$  are the nonperturbative parton distributions, determined from fits to data,  $x_1$  and  $x_2$  are the fractional momentum of hadrons  $A$  and  $B$  carried by partons  $i$  and  $j$ ,  $\tau = s/S$

$\hat{\sigma}_{ij}(s, m^2, \mu_F^2, \mu_R^2)$  is hard partonic cross section calculable in QCD in powers of  $\alpha_s^{2+n}$ : leading order (LO),  $n = 0$ ; next-to-leading order (NLO),  $n = 1 \dots$

Results depend strongly on quark mass,  $m$ , factorization scale,  $\mu_F$ , in the parton densities and renormalization scale,  $\mu_R$ , in  $\alpha_s$

# Choosing Parameters

Two important parameters: the quark mass  $m$  and the scale  $\mu$  – at high energies, far from threshold, the low  $x$ , low  $\mu$  behavior of the parton densities determines the charm result, bottom less sensitive to parameter choice

The scale is usually chosen so that  $\mu_F = \mu_R$ , as in parton density fits, no strict reason for doing so for heavy flavors

Two ways to make predictions:

**Fit to Data (RV, Hard Probes Collaboration):** fix  $m$  and  $\mu \equiv \mu_F = \mu_R \geq m$  to data at lower energies and extrapolate to unknown regions – favors lower  $m$

**Uncertainty Band (Cacciari, Nason and RV):** band determined from mass range,  $1.3 < m < 1.7$  GeV (charm) and  $4.5 < m < 5$  GeV (bottom) with  $\mu_F = \mu_R = m$ , and range of scales relative to central mass value,  $m = 1.5$  GeV (charm) and  $4.75$  GeV (bottom):  $(\mu_F/m, \mu_R/m) = (1,1), (2,2), (0.5,0.5), (0.5,1), (1,0.5), (1,2), (2,1)$  (Ratio is relative to  $m_T$  for distributions)

**Need to be careful with  $\mu_F \leq m$  and the CTEQ6M parton densities since  $\mu_{\min} = 1.3$  GeV, gives big  $K$  factors for low scales – problem occurs at low  $p_T$**

**Densities like GRV98 have lower  $\mu_{\min}$  so low  $x$ , low  $\mu$  behavior less problematic**

**Value of two-loop  $\alpha_s$  is big for low scales, for  $m = 1.5$  GeV:**

$\alpha_s(m/2 = 0.75 \text{ GeV}) = 0.648$ ,  $\alpha_s(m = 1.5 \text{ GeV}) = 0.348$  and  $\alpha_s(2m = 3 \text{ GeV}) = 0.246$

# CTEQ6M Densities at $\mu = m/2$ , $m$ and $2m$

CTEQ6M densities extrapolate to  $\mu < \mu_{\min} = 1.3$  GeV

When backwards extrapolation leads to  $xg(x, \mu) < 0$ , then  $xg(x, \mu) \equiv 0$

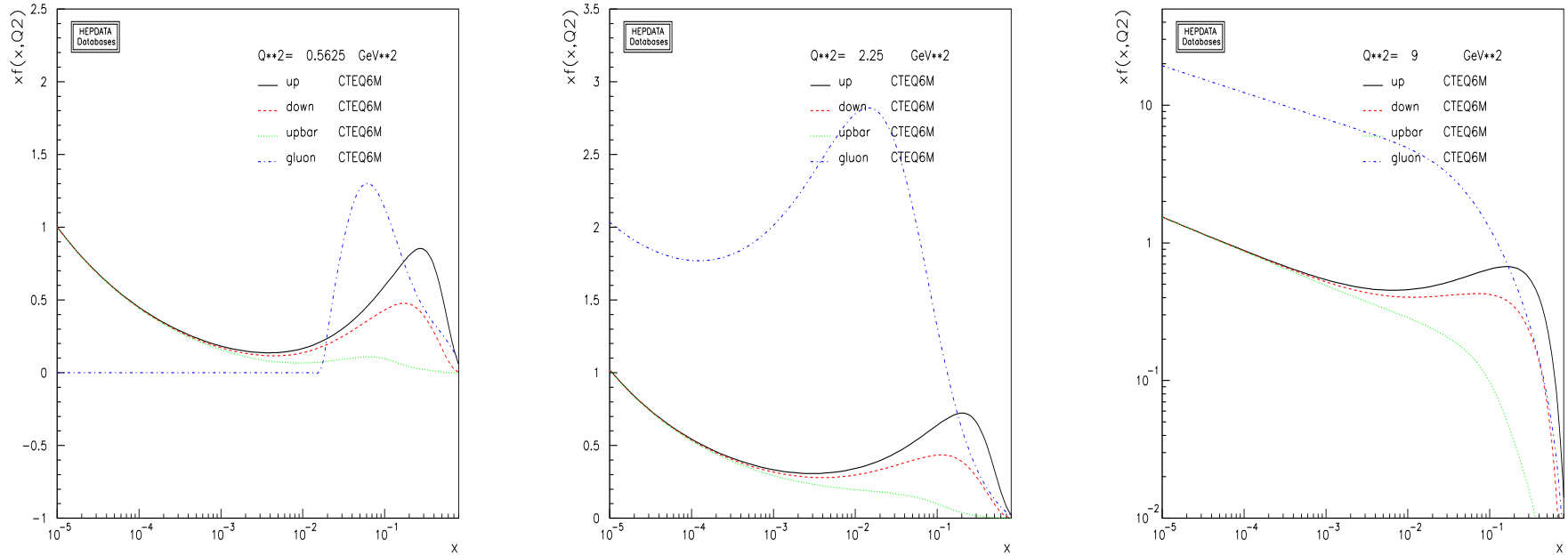


Figure 1: The CTEQ6M parton densities as a function of  $x$  for  $\mu = m/2$  (left),  $\mu = m$  (middle) and  $\mu = 2m$  (right) for  $m = 1.5$  GeV.

# FONLL Calculation (Cacciari and Nason)

Designed to cure large logs of  $p_T/m$  for  $p_T \gg m$  in fixed order calculation (FO) where mass is no longer only relevant scale

Includes resummed terms (RS) of order  $\alpha_s^2(\alpha_s \log(p_T/m))^k$  (leading log – LL) and  $\alpha_s^3(\alpha_s \log(p_T/m))^k$  (NLL) while subtracting off fixed order terms retaining only the logarithmic mass dependence (the “massless” limit of fixed order (FOM0)), both calculated in the same renormalization scheme

Scheme change needed in the FO calculation since it treats the heavy flavor as heavy while the RS approach includes the heavy flavor as an active light degree of freedom

Schematically:

$$\text{FONLL} = \text{FO} + (\text{RS} - \text{FOM0}) G(m, p_T)$$

$G(m, p_T)$  is arbitrary but  $G(m, p_T) \rightarrow 1$  as  $m/p_T \rightarrow 0$  up to terms suppressed by powers of  $m/p_T$

Total cross section similar to but slightly higher than NLO

Problems at high energies away from midrapidity due to small  $x$ , high  $z$  behavior of fragmentation functions in RS result, therefore we don't calculate results for  $|y| > 2$ , worse for LHC predictions

# Comparison of FONLL and NLO $p_T$ Distributions

FONLL result for bare charm is slightly higher over most of the  $p_T$  range – fixed order result gets higher at large  $p_T$  due to large  $\log(p_T/m)$  terms

New  $D^0$  fragmentation functions (dashed) harder than Peterson function (dot-dot-dot-dashed)

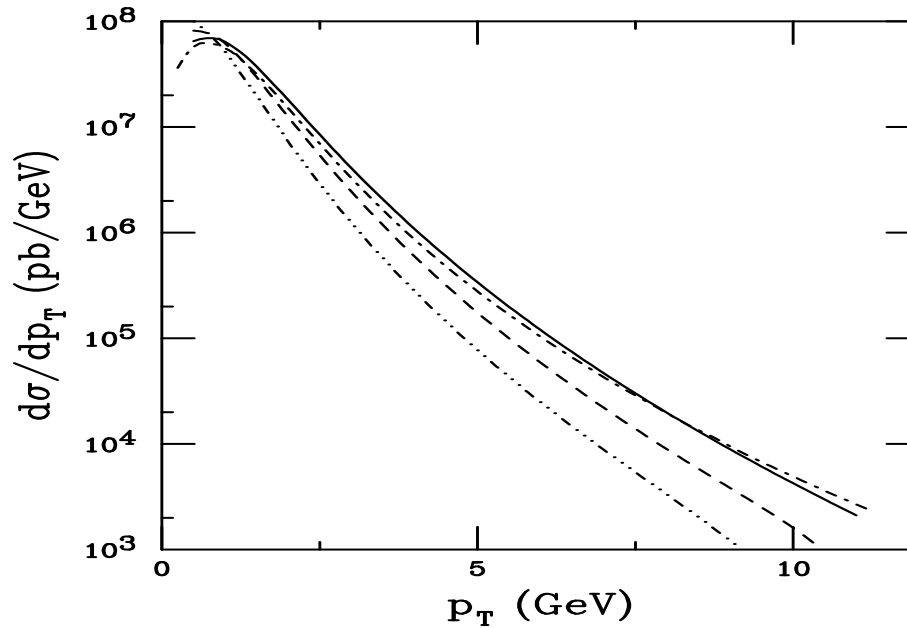


Figure 2: The  $p_T$  distributions calculated using FONLL are compared to NLO. The dot-dashed curve is the NLO charm quark  $p_T$  distribution. The solid, dashed and dot-dot-dot-dashed curves are FONLL results for the charm quark and  $D^0$  meson with the updated fragmentation function and the Peterson function, respectively. All the calculations are done with the CTEQ6M parton densities,  $m = 1.2$  GeV and  $\mu = 2m_T$  in the region  $|y| \leq 0.75$ .

# Uncertainty Bands for $p_T$ Distributions

Due to range of parameters chosen for uncertainty band, the maximum and minimum result as a function of  $p_T$  may not come from a single set of parameters

Thus the upper and lower curves in the band do not represent a single set of  $\mu_R$ ,  $\mu_F$  and  $m$  values but are the upper and lower limits of mass and scale uncertainties added in quadrature:

$$\begin{aligned}\frac{d\sigma_{\max}}{dp_T} &= \frac{d\sigma_{\text{cent}}}{dp_T} + \sqrt{\left(\frac{d\sigma_{\mu,\max}}{dp_T} - \frac{d\sigma_{\text{cent}}}{dp_T}\right)^2 + \left(\frac{d\sigma_{m,\max}}{dp_T} - \frac{d\sigma_{\text{cent}}}{dp_T}\right)^2} \\ \frac{d\sigma_{\min}}{dp_T} &= \frac{d\sigma_{\text{cent}}}{dp_T} - \sqrt{\left(\frac{d\sigma_{\mu,\min}}{dp_T} - \frac{d\sigma_{\text{cent}}}{dp_T}\right)^2 + \left(\frac{d\sigma_{m,\min}}{dp_T} - \frac{d\sigma_{\text{cent}}}{dp_T}\right)^2}\end{aligned}$$

The central values are  $m = 1.5$  GeV (charm) and 4.75 GeV (bottom),  $\mu_F = \mu_R = m_T$   
We follow the same procedure for both the NLO and FONLL calculations and compare them in the central ( $|y| \leq 0.75$ ) and forward ( $1.2 < y < 2.2 - 1.2 < y < 2$  for FONLL) regions

Previous (HPC) charm results with  $m = 1.2$  GeV,  $\mu_F = \mu_R = 2m_T$  fall within the uncertainty band

Bare heavy quark and heavy flavor meson  $p_T$  distributions shown for  $pp$  collisions at  $\sqrt{S} = 200$



# Components of Uncertainty Band at NLO

Curves with  $(\mu_F/m_T, \mu_R/m_T) = (1, 0.5)$  and  $(0.5, 0.5)$  define the maximum of the band with  $(0.5, 1)$  and  $(2, 2)$  form the minimum

Turnover of minimum at low  $p_T$  because  $\mu_F < \mu_{\min}$  of CTEQ6M

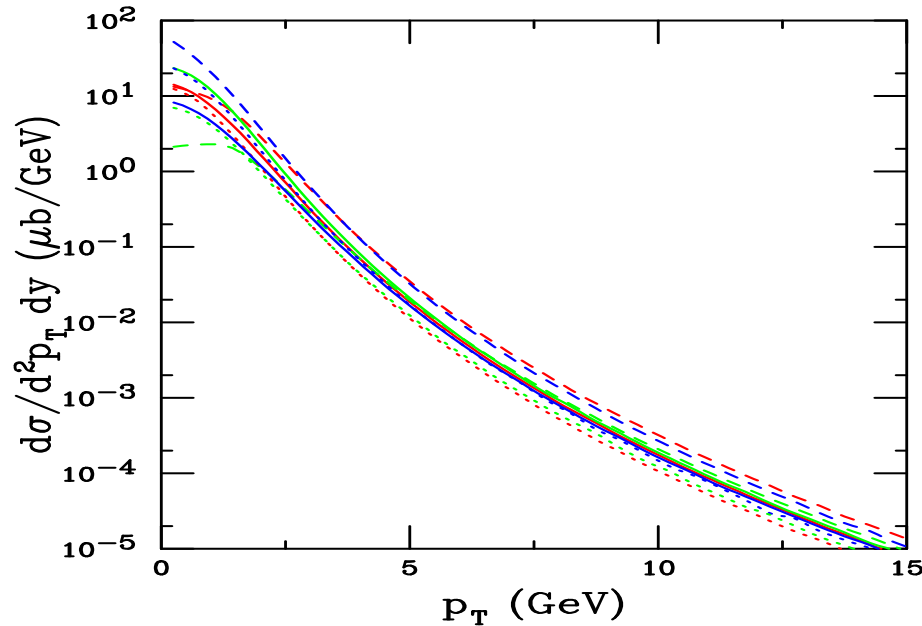


Figure 3: The charm quark  $p_T$  distributions calculated using CTEQ6M. The solid red curve is the central value  $(\mu_F/m_T, \mu_R/m_T) = (1, 1)$  with  $m = 1.5$  GeV. The green and blue solid curves are  $m = 1.3$  and  $1.7$  GeV with  $(1, 1)$  respectively. The red, blue and green dashed curves correspond to  $(0.5, 0.5)$ ,  $(1, 0.5)$  and  $(0.5, 1)$  respectively while the red, blue and green dotted curves are for  $(2, 2)$ ,  $(1, 2)$  and  $(2, 1)$  respectively, all for  $m = 1.5$  GeV.

# Uncertainty Bands for $c$ and $D$ at 200 GeV

NLO and FONLL bands very similar to each other

$D$  meson band calculated for primary  $D$ s

Not possible to separate  $c$  and  $D$  bands for  $p_T < 10$  GeV – looks more like a delta function

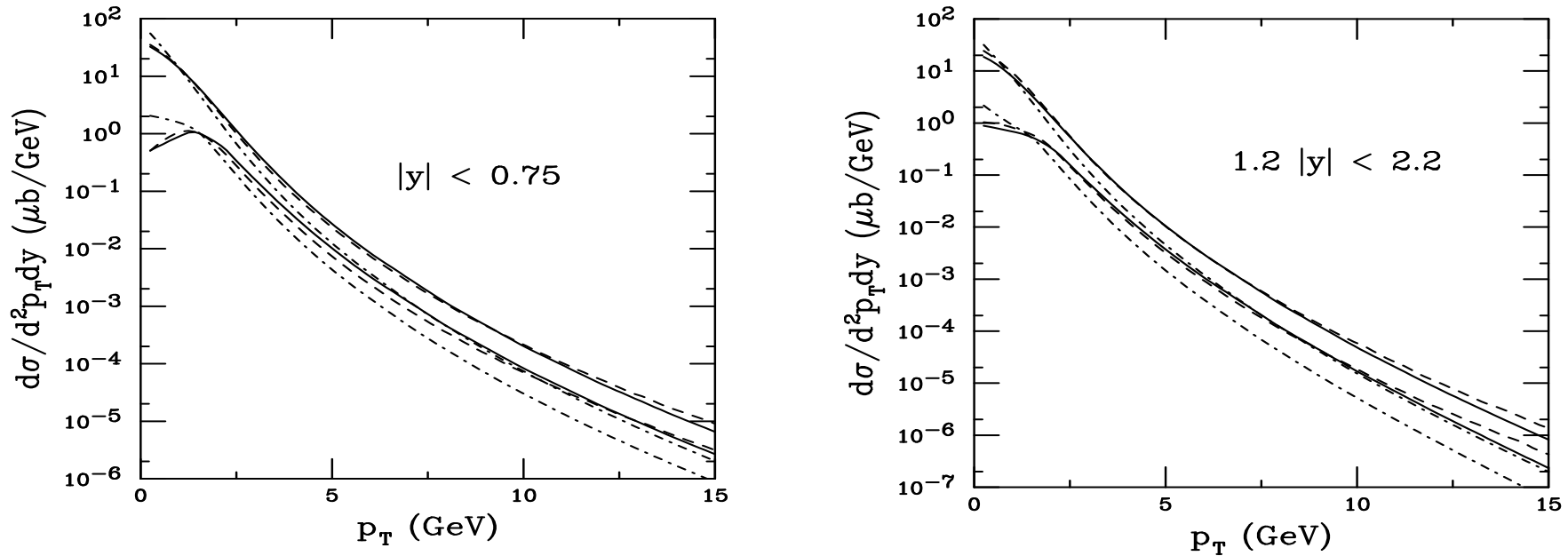


Figure 4: The charm quark theoretical band as a function of  $p_T$  for FONLL (solid curves) and NLO (dashed curves) in  $\sqrt{S} = 200$  GeV  $pp$  collisions. Also shown is the  $D$  meson uncertainty band, all using the CTEQ6M parton densities. The left-hand plot gives the result for  $|y| \leq 0.75$  while the right-hand plot shows the result for  $1.2 \leq |y| \leq 2.2$ .

# Comparison to STAR d+Au $D$ Data

Agreement of upper limit of uncertainty band with low  $p_T$  STAR data rather reasonable

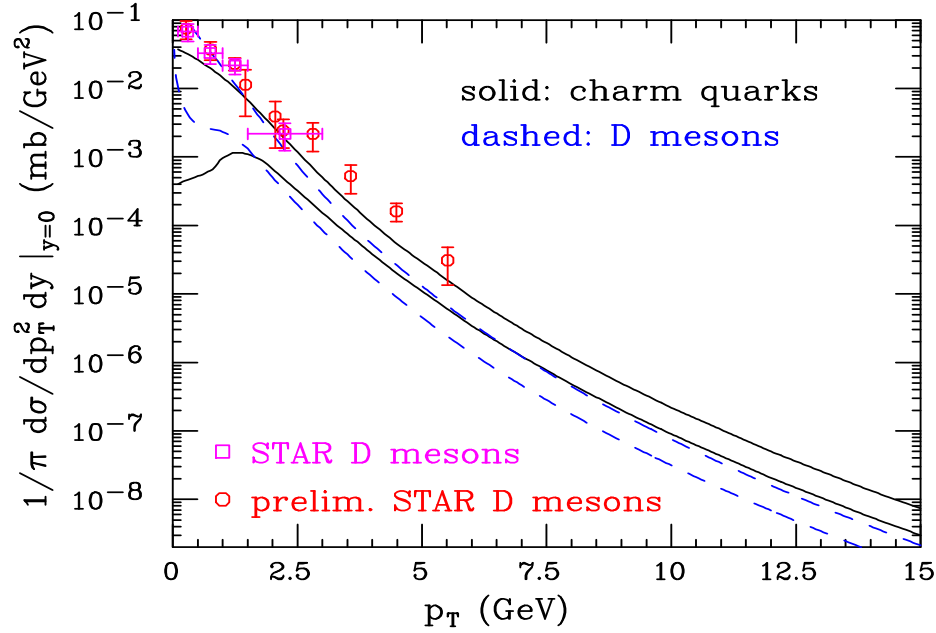


Figure 5: The FONLL theoretical uncertainty bands for the charm quark and  $D$  meson  $p_T$  distributions in  $pp$  collisions at  $\sqrt{S} = 200$  GeV, using  $\text{BR}(c \rightarrow D) = 1$ . Both final and preliminary STAR d+Au data (scaled to  $pp$  using  $N_{\text{bin}} = 7.5$ ) at  $\sqrt{S_{NN}} = 200$  GeV are also shown.

# Uncertainty Bands for $b$ and $B$ at 200 GeV

Bands narrower for bottom than for charm

Impossible to separate  $b$  from  $B$  over the  $p_T$  range shown ( $B$  is a generic  $B$  meson)

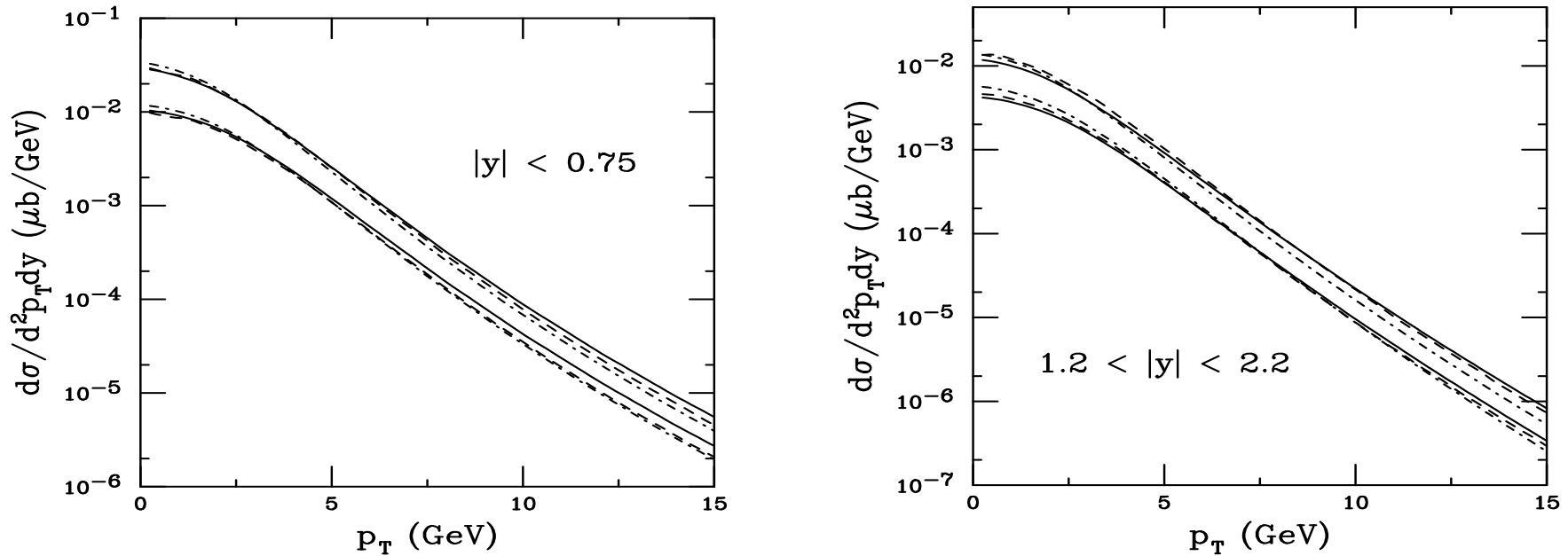


Figure 6: The bottom quark theoretical band as a function of  $p_T$  for FONLL (solid curves) and NLO (dashed curves) in  $\sqrt{S} = 200$  GeV  $pp$  collisions. Also shown is the  $B$  meson uncertainty band, all using the CTEQ6M parton densities. The left-hand plot gives the result for  $|y| \leq 0.75$  while the right-hand plot shows the result for  $1.2 \leq |y| \leq 2.2$ .

# Obtaining the Electron Spectra From Heavy Flavor Decays

$D$  and  $B$  decays to leptons depends on measured decay spectra and branching ratios

$D \rightarrow e$  Use preliminary CLEO data on inclusive electrons from semi-leptonic  $D$  decays, assume it to be identical for all charm hadrons

$B \rightarrow e$  Primary  $B$  decays to electrons measured by Babar and CLEO, fit data and assume fit to work for all bottom hadrons

$B \rightarrow D \rightarrow e$  Obtain electron spectrum from convolution of  $D \rightarrow e$  spectrum with parton model calculation of  $b \rightarrow c$  decay

Branching ratios are admixtures of charm and bottom hadrons

$$B(D \rightarrow e) = 10.3 \pm 1.2 \%$$

$$B(B \rightarrow e) = 10.86 \pm 0.35 \%$$

$$B(B \rightarrow D \rightarrow e) = 9.6 \pm 0.6 \%$$

# Uncertainty Bands for Electrons from Heavy Flavor Decays at 200 GeV

Electrons from  $B$  decays begin to dominate at  $p_T \sim 5$  GeV

Electron spectra very sensitive to rapidity range – to get  $|y| \leq 0.75$  electrons, need  $|y| \leq 2$  charm and bottom range

Forward electron spectra thus not possible to obtain using FONLL code due to problems at large  $y$

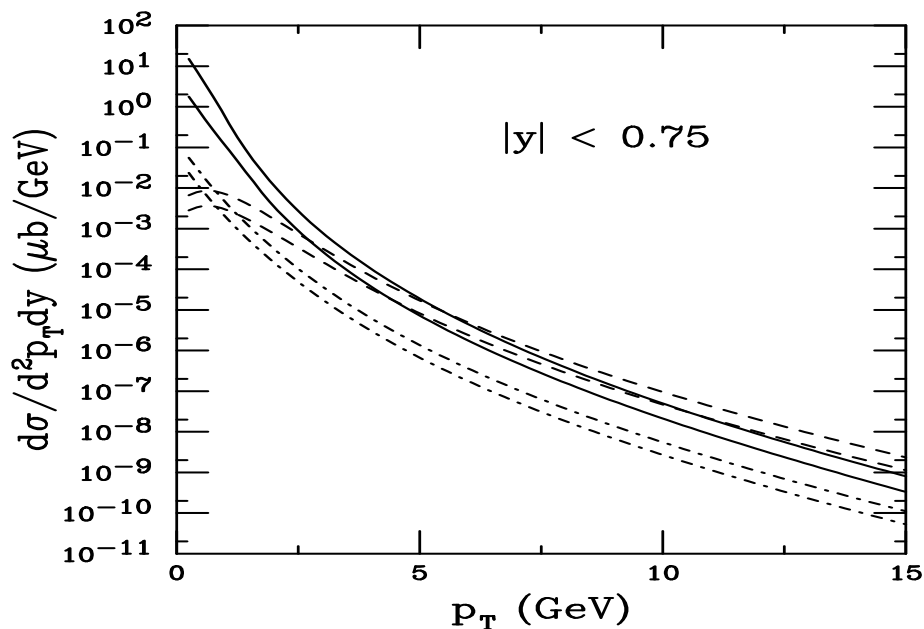


Figure 7: The theoretical FONLL bands for  $D \rightarrow eX$  (solid),  $B \rightarrow eX$  (dashed) and  $B \rightarrow DX \rightarrow eX'$  (dot-dashed) as a function of  $p_T$  in  $\sqrt{S} = 200$  GeV  $pp$  collisions for  $|y| < 0.75$ .

# Comparison to Electron Data at 200 GeV

Includes PHENIX preliminary data from  $pp$  and STAR published and preliminary data

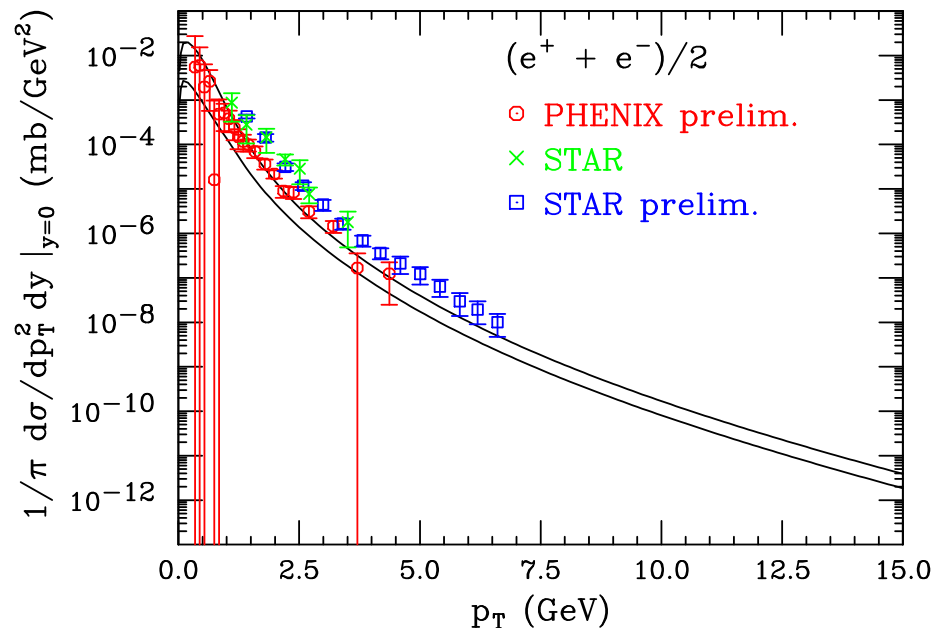


Figure 8: Prediction of the theoretical uncertainty band of the total electron spectrum from charm and bottom (Cacciari, Nason and RV). Preliminary data from PHENIX and STAR are also shown.

## Summary .

- The FONLL calculation of heavy quark production is used to better predict the  $p_T$  dependence at collider energy – cures large logs of  $p_T/m$
- Includes more modern fragmentation functions for  $D$  and  $B$  mesons – meson and quark distributions similar at higher  $p_T$  than previously obtained from older  $e^+e^-$  fits .
- Contributions of  $D$  and  $B$  decays to leptons difficult to disentangle, requires reconstruction of hadronic decays to distinguish between them